Single Difference Code-based Technique for Direct Position Estimation

Shuo Tang *Dept. of Electrical and Computer Engineering, Northeastern University*
Haoqing Li, *Department of Geomatics Engineering, University of Calgary*
Pau Closas *Dept. of Electrical and Computer Engineering, Northeastern University*

BIOGRAPHY

Shuo Tang got his BS degree in Vehicle Engineering from China Agricultural University, China and MS degree in Mechanical Engineering at Northeastern University. He is currently a PhD student in Electrical Computer Engineering at Northeastern University, Boston, MA. His research interest focuses on satellite signal processing, positioning and navigation, physics-based learning and computational statistics.

Haoqing Li received his BS degree in electrical engineering from Wuhan University, China, in 2016 and an MS and PhD in electrical and computer engineering from Northeastern University, Boston, MA, in 2018 and 2023, respectively. Currently he is a postdoctoral associate in the Position, Location and Navigation (PLAN) Group at the University of Calgary. His research interests include Global Navigation Satellite System (GNSS) signal processing, interference mitigation techniques, satellite image processing, Bayesian filtering, deep learning, and robust statistics.

Pau Closas is Associate Professor at Northeastern University, Boston, MA. He received the MS and PhD degrees in Electrical Engineering from UPC in 2003 and 2009. He also holds a MS in Advanced Mathematics from UPC, 2014. His primary areas of interest include statistical signal processing, robust stochastic filtering, and machine learning, with applications to positioning systems and wireless communications. He is the recipient of the 2014 EURASIP Best PhD Thesis Award, the 9th Duran Farell Award, the 2016 ION Early Achievements Award, and a 2019 NSF CAREER Award.

ABSTRACT

Global Navigation Satellite System (GNSS) has been widely used in navigation and positioning applications, where precise position and time estimation are required. Conventional GNSS positioning methods require a two-step (2SP) process, where intermediate measurements such as Doppler shift and time delay of received signals are computed and then used to solve for the receiver position. Alternatively, to acquire superior levels of sensitivity and operation under challenging environments, Direct Position Estimation (DPE) was proposed to estimate the position directly from the received signal without intermediate variables. However, the positioning resilience of DPE method is still under the influence of common error and bias terms, like the satellite clock bias, ionospheric error and tropospheric error. In conventional 2SP method, Differential Global navigation satellite system (DGNSS) technique is commonly used to improve GNSS positioning accuracy, among which the Single Difference (SD) between two receivers can help remove satellite clock bias, ionosphere and troposphere errors. With current DPE research focusing on a single receiver, this paper introduces SD approach to the DPE scheme, using SD code observations to reduce influence from satellite clock bias, ionospheric error and tropospheric error. Simulations and experiments have been carried out to demonstrate and validate the efficiency of the proposed method compared to the standard DPE approach, in terms of a smaller RMSE of positioning solutions.

I. INTRODUCTION

Global navigation satellite system (GNSS) provides positioning, navigation and timing solutions by utilizing transmitted signals from satellites. The traditional method of GNSS positioning is usually recognized as a two-step (2SP) method since the GNSS observables, such as pseudorange, pseudorange rate and carrier phase, are first estimated by the receiver during acquisition and tracking stage. Then those observables will be employed by weighted least squares (WLS) or Kalman Filter (KF) to solve the unknown position, velocity and time (PVT). Many techniques have been developed based on these two stages in the past decades. For example, the discriminator design for delay locked loop (DLL) and phase locked loop (PLL) improve the tracking performance. The real-time kinematic (RTK) and precise point positioning (PPP) introduces phase observation and ambiguity integer resolution to improve the positioning precision. The robust filtering techniques detect and reduce the performance degrade brought by outlier measurement. Those techniques are described in many famous GNSS textbooks [Kaplan and Hegarty, 2017, Hofmann-Wellenhof et al., 2007, Borre et al., 2007, Groves, 2013, Tsui, 2005], which make 2SP the most mature and classical GNSS positioning approach.

Among many advanced techniques, differential GPS (DGPS) is one of the most popular methods due to the wide distribution

of the base station and cheap access of data from the commercial receiver. The DGPS refers to the method which leverages the GPS observables or other correct information from one or more reference stations at known locations to improve the positioning or timing performance [Kaplan and Hegarty, 2017]. The information provided by the base stations includes raw GNSS measurements (e.g. pseudorange and carrier phase), corrections to raw GNSS measurement or ephemeris information, integrity data and the other auxiliary data (e.g. the accurate location of the base station). The common differential techniques operate in measurement domain, e.g. difference between two pseudorange measurements (code-based positioning) or two carrier phase measurements (phase-based positioning). The core idea of the differential techniques is that the difference between two measurements may remove the common error terms and thus improve the accuracy of the observables. For example, the single difference (SD) between two pseudorange measurements, collected from two short-baseline receivers but with respect to the same satellite at the same moment, eliminates the common ionosphere and troposphere errors and the clock bias of the satellites. The double difference (DD), achieved by differencing two SD measurements for different satellites, will further remove the clock bias of receivers. The DD is a basis of RTK method [Langley, 1998], which is one of the most popular precise navigation methods. It can achieve centimeter-level precision in real time, making it essential for applications that require high-accuracy positioning. Besides, the between-satellite SD has been using in PPP to overcome drawbacks of conventional PPP models [Elsobeiey and El-Rabbany, 2014]. The between-receiver SD is used for spoofing detection [Xiao et al., 2016], and precise positioning [Liu et al., 2004]. Furthermore, a modified version of between-receiver SD is designed in [Gao et al., 2022] for RTK to detect and exclude fault. In this paper, we focus on the between-receiver SD as a beginning of the combination of DGPS techniqes with direct position estimation (DPE) scheme.

Recently, DPE arises more and more interest since its high-sensitivity (HS) enables better positioning performance in the harsh environment. Unlike the traditional 2SP method, DPE solves for the PVT from the raw satellite signal without estimating intermediate quantities, such as pseudorange and carrier phase. A DPE receiver fuses the information from visible satellites at the early stage of processing and thus increases its sensitivity to utilize weak signals. In the GNSS context, DPE was first proposed in [Closas et al., 2007], and recently revisited in [Closas and Gusi-Amigo, 2017] and [Morton et al., 2021, Ch. 21]. From both theoretical analysis [Closas et al., 2009, Gusi-Amigó et al., 2014, Gusi-Amigó et al., 2018] and practical experiments [Dampf et al., 2019, Tang et al., 2023], it has been shown that the DPE approach has a better performance than the tradition method in terms of precision and robustness under unfavorable environment.

The DPE approach has never been combined with the DGPS methodologies before, but thanks to the development of the portable GNSS devices and the software-defined radio (SDR) paradigm, it is possible to access multiple raw received signals and treat one of them as the reference station with a known location. Our contribution in this work is to develop a differential approach (e.g. code-based SD) for DPE by utilizing the raw satellite signal from the receivers to correct the common iono/troposhpere error. Based on the core idea of DPE to operate the receiver signal in the navigation domain, we are also going to propose a signal reconstruction method for the reference signal to degrade the noise floor brought by the cross correlation between different satellites. The proposed Single Difference Direct Position Estimation (SD-DPE) approach is expected to keep the high-sensitive property of the standard PDE approach and improve positioning performance compared to standard DPE by removing the common error terms, e.g. the iono/troposphere error, from satellite signal given the observables from the other short-baseline receiver.

The remaining paper is organized as following:

- Section II starts with the SD technique and the DPE approach. After that, we are going to introduce our main idea of removing the common error, such as iono/troposphere error in signal level. Then we will propose our SD-DPE approach by reconstructing the signal from reference receiver and defining the cost function for searching the baseline vector.
- Section III implements the proposed SD-DPE approach under different conditions, such as the quality of the rover received signal and the uncertainty of the reference measurements. We also provide a practical experiment, with the over-the-air I&Q signal records and the zero-baseline reference receiver, to validate the approach.
- Section IV concludes the positioning performance of the proposed approach with a given reference receiver. The SD-DPE can effectively correct the common error between the rover and reference according to the simulation and experiment results.

II. METHODOLOGY

1. Single difference observations

The pseudorange from i-th satellite to r-th receiver is modeled as:

$$\rho_r^i = ||\boldsymbol{p}_r - \boldsymbol{p}^i|| + c(dt_r - dt^i) + \delta I_r^i + \delta T_r^i + \epsilon_r^i \tag{1}$$

where the subscript $r \in \{1, 2\}$ denotes two receivers and the superscript $i \in \{1, 2, \cdots, M\}$ denotes each common satellite for the receivers, $\boldsymbol{p}_r$ and dt_r denote the position and clock offset of the r-th receiver, $\boldsymbol{p}^i$ and dt^i denote the position and clock offset of the ith satellite, δI_r^i and δT_r^i denote the ionosphere and troposphere error, c denotes the speed of light and ϵ denotes the other unmodeled error term (e.g. relativistic effects). With an assumption that $\delta I_1^i = \delta I_2^i$ and $\delta T_1^i = \delta T_2^i$, between-receiver SD observation is defined as:

$$\triangle\rho_r^i = \rho_1^i - \rho_2^j = ||\boldsymbol{p}_1 - \boldsymbol{p}^i|| - ||\boldsymbol{p}_2 - \boldsymbol{p}^i|| + c(dt_1 - dt_2) + \epsilon_1^i - \epsilon_2^i \tag{2}$$

By using the SD measurements as observation for positioning, we can reduce the influence of common error terms: ionospheric error, tropospheric error, and satellite clock bias.

2. Direct position estimation

In conventional two-step positioning method, the received signal of r-th receiver after sampling can be modeled as:

$$x_r[k] = \sum_{i=1}^{M} a_r^i s^i(kT_s - \tau_r^i) \exp\left(j2\pi f_{d,r}^i kT_s + \phi_r^i\right) + n_r(t). \tag{3}$$

where $T_s = \frac{1}{f_s}$ is the sampling period, f_s is the sampling frequency, a denotes the complex amplitude of the signal, $s(t)$ is the navigation signal spread through PRN code, τ is the time-delay from the satellite to the receiver, f_d is the Doppler-shift, ϕ_r^i represents the phase information, and $n_r(t) \sim \mathcal{N}(0, \sigma_{n,r}^2)$ denotes a complex additive white Gaussian noise (AWGN) process which includes unmodeled terms besides line-of-sight (LOS) signals. Given that we focused on code measurements only by maximizing standard CAF, the phase information ϕ_r^i can be ignored, leading to Eq.(3) updated as:

$$x_r[k] = \sum_{i=1}^{M} a_r^i s^i(kT_s - \tau_r^i) \exp\left(j2\pi f_{d,r}^i kT_s\right) + n_r(t). \tag{4}$$

For positioning purpose, we need to estimate two intermediate variables τ_r^i and $f_{d,r}^i$:

$$\begin{aligned} \{\tau_r^i . f_{d,r}^i\} &= \underset{\{\tau_r^i \cdot f_{d,r}^i\}}{\arg\max}\, Y_i(\tau_r^i . f_{d,r}^i) \\ &= \underset{\{\tau_r^i \cdot f_{d,r}^i\}}{\arg\max} \left| \sum_{k=0}^{K} x_r[kT_s] s^i(kT_s - \tau_r^i) \exp\left(-j2\pi f_{d,r}^i kT_s\right) \right|^2 \end{aligned} \tag{5}$$

where $Y_i(\tau_r^i . f_{d,r}^i) = \left| \sum_{k=0}^{K} x_r[kT_s] s^i(kT_s - \tau_r^i) \exp\left(-j2\pi f_{d,r}^i kT_s\right) \right|^2$ is defined as Cross Ambiguity Function (CAF). With the two intermediate variables estimated, we can achieve observations for positioning purpose.

However, the use of intermediate variables brings additional uncertainty to positioning accuracy. To improve its performance, DPE approach is proposed [Closas et al., 2007, Closas and Gusi-Amigo, 2017]. A general description is provided in this subsection. In the standard DPE method, we model the time delay and Doppler shift as a function of position and velocity of receiver:

$$\tau_r^i = \frac{1}{c}(||\boldsymbol{p}_r - \boldsymbol{p}^i|| + c(dt_r - dt^i)) \tag{6}$$

$$f_{d,r}^i = -(\boldsymbol{v}^i - \boldsymbol{v}_r)^\top \boldsymbol{u}_r^i \frac{f_c}{c}, \tag{7}$$

where c represents the speed of light, $\boldsymbol{v}^i$ is the velocity of the ith satellite and $\boldsymbol{v}_r$ is the velocity of the receiver. $\boldsymbol{u}_r^i$ denotes the unit vector pointing from the receiver to the satellite i

$$\boldsymbol{u}_r^i = \frac{\boldsymbol{p}^i - \boldsymbol{p}_r}{||\boldsymbol{p}^i - \boldsymbol{p}_r||}. \tag{8}$$

Thus, we can reparameterize Eq.(4) as:

$$x_r[k] = \sum_{i=1}^{M} a_r^i s^i(kT_s - \tau_r^i(\boldsymbol{p}_r)) \exp\left(j2\pi f_{d,r}^i(\boldsymbol{p}_r, \boldsymbol{v}_r)kT_s\right) + n_r(t), \tag{9}$$

and the positioning solution can be achieve by maximizing a summation of CAF:

$$\begin{aligned}\{\boldsymbol{p}_r, \boldsymbol{v}_r\} &= \arg\max_{\{\boldsymbol{p}_r, \boldsymbol{v}_r\}} \sum_{i=1}^{M} Y_i(\tau_r^i(\boldsymbol{p}_r), f_{d,r}^i(\boldsymbol{p}_r, \boldsymbol{v}_r)) \\ &= \arg\max_{\{\boldsymbol{p}_r, \boldsymbol{v}_r\}} \sum_{i=1}^{M} \left| \sum_{k=0}^{K} x_r[kT_s] s^i(kT_s - \tau_r^i(\boldsymbol{p}_r)) \exp\left(-j2\pi f_{d,r}^i(\boldsymbol{p}_r, \boldsymbol{v}_r)kT_s\right) \right|^2 \end{aligned} \tag{10}$$

However, the standard DPE does not consider the ionospheric and tropospheric errors, and therefore influenced by those two errors. To reduce the influence, an SD-DPE method is proposed in this paper and presented in subsection II.3.

3. Proposed method

Unlike the standard DPE approach, in the SD-DPE method, we have two receivers for the SD scheme. Considering two static short-baseline receivers, the dynamics of the receiver which we are interested in is the position $\boldsymbol{p}$, clock offset dt.

Note that we assume $\boldsymbol{u}_1^i \approx \boldsymbol{u}_2^i$ due to the short-baseline setting. It is noted that the Doppler-shift and velocity of the receiver is temporarily ignored since *1)* the velocity is out of the interest of the this work and the estimation of the velocity can be decoupled from the estimation of the position [Chu et al., 2019]; *2)* in DGPS method, one of the receiver is likely to be a static reference receiver, which means the Doppler-shift $f_{d,1}^i$ and $f_{d,2}^i$ should be close; and *3)* in the correlation we are going to perform later, the slight difference of the Doppler-shift will only influence the noise floor and the correlation value, but not the position of the peak.

Assuming the avaliable satellites to both receivers are the same, we can have the CAF $Y(\tau)$ as shown below

$$Y(\tau) = \left| \sum_{k=0}^{K} x_1[kT_s] x_2^*[kT_s - \tau] \right|^2 \tag{11}$$

where $*$ means the conjugate operator and the received signals of two receivers are written in a discrete form with the sampling rate $f_s = 1/T_s$ and K denotes the number of the samples in a coherent integration time. One can notice that the peaks of $Y(\tau)$ will appear at $\tau = \{\tau_{12}^1, \ldots, \tau_{12}^M\}$, where $\tau_{12}^i = \tau_2^i - \tau_1^i$ is the difference of the delay/pseudorange of the two receivers with respect to the ith satellite and M is the number of the common satellites shared by two receivers.

Note that τ_{12}^i can be expressed as a function of the baseline vector $\vec{\boldsymbol{b}}$ between receiver 1 and 2,

$$\tau_{12}^i(\vec{\boldsymbol{b}}) = \frac{\vec{\boldsymbol{b}}\boldsymbol{u}_1^i}{c}, \tag{12}$$

where the receiver 1 is considered to be a reference receiver with a given position, which means the unit vector $\boldsymbol{u}_1^i$ is known to us. It is noted that those delays/pseudoranges are the function of the baseline vector $\vec{\boldsymbol{b}}$ and they have got rid of the ionospheric and tropospheric errors due to the differential operation. To this end, we can find the baseline vector $\vec{\boldsymbol{b}}$ by solving the following optimization problem in DPE context

$$\vec{\boldsymbol{b}} = \arg\max_{\vec{\boldsymbol{b}}} \sum_{i=1}^{M} Y(\tau_{12}^i(\vec{\boldsymbol{b}})). \tag{13}$$

Thus the position of the receiver 2 can also be estimated as $\boldsymbol{p}_2 = \boldsymbol{p}_1 + \vec{\boldsymbol{b}}$ without ionosphere and troposphere error.

However, the correlation operation brings noise to the CAF $Y(\tau)$ [Borio, 2008],and the cross-correlation of the C/A codes from two satellites is also regarded as noise. This noise source increases when the number of satellites increases [Arribas et al., 2010], which will raise the noise floor and make it difficult to distinguish the peaks on the CAF.

A solution to this challenge is to consider one of the receivers as a base station and reconstruct the received signal from its GNSS observables. Doing this will not degrade the HS property of the DPE approach since the DPE optimization still happens in the navigation domain of the other receiver. Also, the GNSS measurements from a base station are usually collected under benign environment with high carrier-to-noise ratio and no multipath effect. Besides, reconstruction of the signal has more advantages over using raw received signal: *a)* the received signal can be reconstructed for each satellite and separately perform correlation with the signal from the other receiver before the summation, which circumvents the noise caused by cross correlation between different satellites; *b)* the common error, such as ionosphere and troposphere error, is still included in the observables, which still enables the DGPS technique after signal reconstruction; *c)* the base stations are widely distributed and its GNSS measurements are easy to access, which could help realize and popularize DGPS DPE algorithm.

Therefore, Eq.(13) can be updated as:

$$\begin{aligned}\vec{\boldsymbol{b}} &= \arg\max_{\vec{\boldsymbol{b}}} \sum_{i=1}^{M} \tilde{Y}(\tau_{12}^{i}(\vec{\boldsymbol{b}})) \\ &= \arg\max_{\vec{\boldsymbol{b}}} \sum_{i=1}^{M} \left| \sum_{k=0}^{K} \tilde{x}_1^i[kT_s] x_2^*[kT_s - \tau_{12}^i(\vec{\boldsymbol{b}})] \right|^2 \end{aligned} \tag{14}$$

where $\tilde{x}_1^i = s^i(kT_s - \tilde{\tau}_1^i)\exp\left(-j2\pi\tilde{f}_{d,1}^i kT_s\right)$ represents the reconstruction of signal from receiver 1 using its GNSS observables $\tilde{\tau}_1^i$ and $\tilde{f}_{d,1}^i$, and $\tilde{Y}$ means the correlation between the reconstructed signal from receiver 1 and the received signal from receiver 2. As stated in [Closas and Gusi-Amigo, 2017, Tang et al., 2023, Vicenzo et al., 2023], the grid-based search or stochastic optimization method can be employed to search the solution of the above cost function. In this paper, we use the so-called Acceleration Random Search (ARS) [Appel et al., 2004] in the following simulations and experiments.

III. SIMULATIONS AND EXPERIMENTS

1. Raw Signal Vs Reconstructed Signal

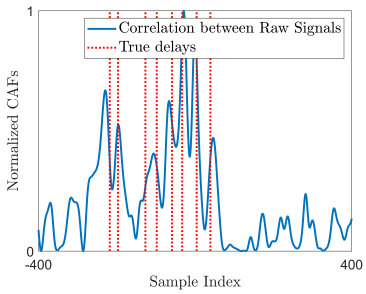

(a) Correlation using the raw signal under $C/N_0 = 50$dB-Hz.

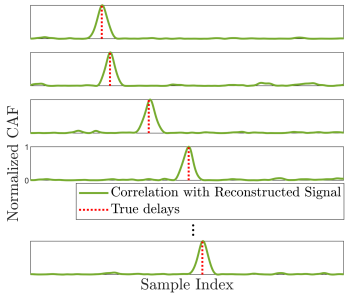

(b) Correlation using the reconstructed signal under $C/N_0 = 50$dB-Hz.

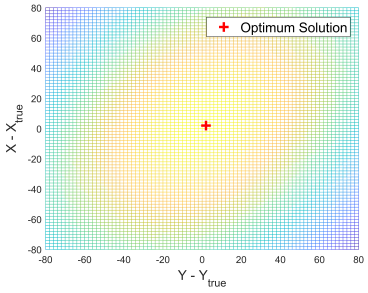

(c) CAF in the navigation domain under $C/N_0 = 50$dB-Hz.

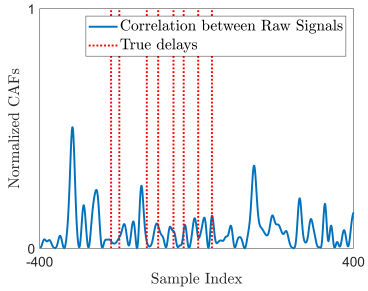

(d) Correlation using the raw signal under $C/N_0 = 40$dB-Hz.

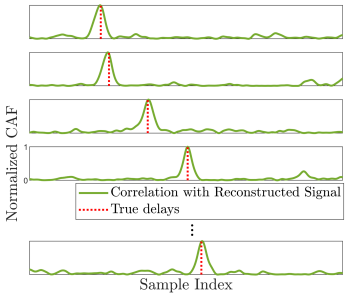

(e) Correlation using the reconstructed signal under $C/N_0 = 40$dB-Hz.

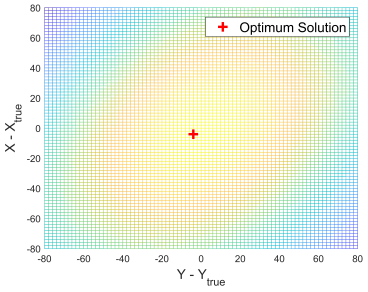

(f) CAF in the navigation domain under $C/N_0 = 40$dB-Hz.

Figure 1: The correlation results with the raw signal and reconstructed with $C/N_0 = 50$dB-Hz (upper row) and $C/N_0 = 40$dB-Hz (lower row). The left and middle column represents the CAF in delay domain. The middle one is plotted for each satellite since the CAF with the reconstructed signal is computed separately for each satellite. The right column plots the CAF in navigation domain.

As proposed, instead of performing correlation between the raw signals sampled by the reference station and rover receiver, we use the observables from the reference station to reconstruct the received signal. By doing this, we can perform the correlation of each satellite individually and avoid the extra noise floor brought by the cross correlation between two different satellites. The reconstruction signal ensures the occurrence of a sharp peak in CAFs, and hence the precision of the position estimation, especially under relative low carrier-to-noise ratio (C/N_0) conditions. For example, Fig 1 shows the correlation results with the raw signal or reconstructed signal from the reference station under C/N_0 $=$ 50dB-Hz and C/N_0 $=$ 40dB-Hz , given 8 common visible satellites for two receivers. The left column represents the CAF from Eq.(11) of two raw signals and the red lines denote the difference of delays τ_{12}^i, where the peaks should appear. The middle column represents the CAFs using reconstructed signals. The right column represents the CAF (using reconstructed signals) in navigation domain centered at the true position in the context of DPE. Remember that the DPE approach will search the position solution directly on this CAF, rather than estimating the delays in the middle column and then deriving the solution.

When C/N_0 $=$ 50dB-Hz, the peaks of the correlations with both raw signal and reconstructed signal are obvious. When C/N_0 $=$ 40dB-Hz, the peaks vanish in the CAF with the raw signal, while there still exist sharp peaks in the CAFs with the reconstructed signals, which helps maintain a good shape of the CAF in navigation domain.

2. The performance of SD-DPE in Different Conditions

The proposed SD-DPE approach needs the raw signal from the user and the observables from the reference receiver to correct the common ionospheric and tropospheric error. One can imagine that the positioning performance may depends on the value of iono/tropospheric errors, the uncertainty of the measurements from the reference and the quality of the raw signal from the rover, which can be parameterized by ionosphere error in meter δI_r^i, troposphere error in meter δT_r^i, estimation standard deviation σ_ρ of the reference measurement and C/N_0 of the rover received signal. Fig. 2 compares the positioning error between DPE and SD-DPE with the existence of ionosphere and troposphere errors. Total 8 satellites were set to be commonly visible by the reference and rover receiver. The rover received the GPS L1 band signal at 40.96MHz sampling rate. The distance between the two receivers were set be be around 1.6km. The ionosphere and troposphere error were set to be Gaussian distributed and assumed to have slight difference between two receivers, e.g. $\delta I_r^i \sim \mathcal{N}(\mu_I, \sigma_I^2)$. All positioning errors are computed as the root mean square error (RMSE) over 400 Monte Carlo simulations. The basis parameters are $\mu_I = 10$m, $\sigma_\rho = 1$m and C/N_0 $=$ 45dB-Hz, which means when one of the parameters is changing, the other two will stay at the fixed value.

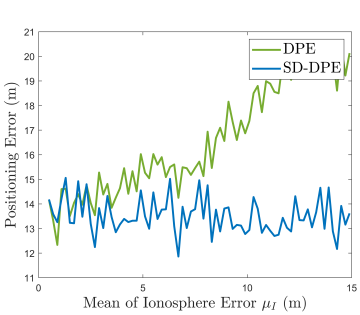

(a) Varying ionospheric error.

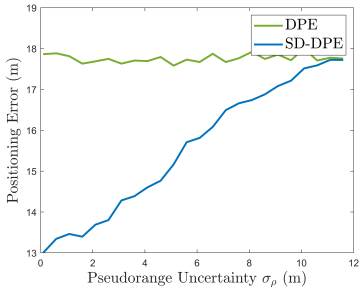

(b) Varying pseudorange uncertainty of the reference station measurement.

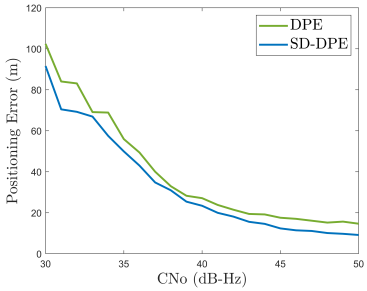

(c) varying C/N_0 of the rover received signal.

Figure 2: Comparison of the positioning performance between DPE and SD-DPE under varying environments.

Fig. 2a shows the positioning errors with respect to the ionosphere error. Since the troposphere error influences the pseudorange in the same way as the ionosphere error does, only the varying ionosphere error is demonstrated here. When the ionosphere error increases, the positioning error of the standard DPE increases, while the one of SD-DPE keeps at the same level. This means our propose approach effectively corrects the ionosphere error with the information from the reference station. Fig. 2b shows that the DPE positioning performance never changes with the pseudorange uncertainty of the reference measurement, since it contains no information from the reference receiver. The positioning error of SD-DPE increases with the uncertainty of the pseudorange, but it only reaches the same error level with the DPE when $\sigma_\rho = 12$m. This is not likely to happen in real-world if the reference receiver is correctly configured, especially for those base stations set under GNSS-favorable environment. Fig. 2c plots how positioning error of DPE and SD-DPE will increase when C/N_0 of the received signal decreases. It is shown that although the positioning performance degrades when rover signal quality becomes worse, the SD-DPE can always correct the iono/troposphere error and get a better positioning result than standard DPE does.

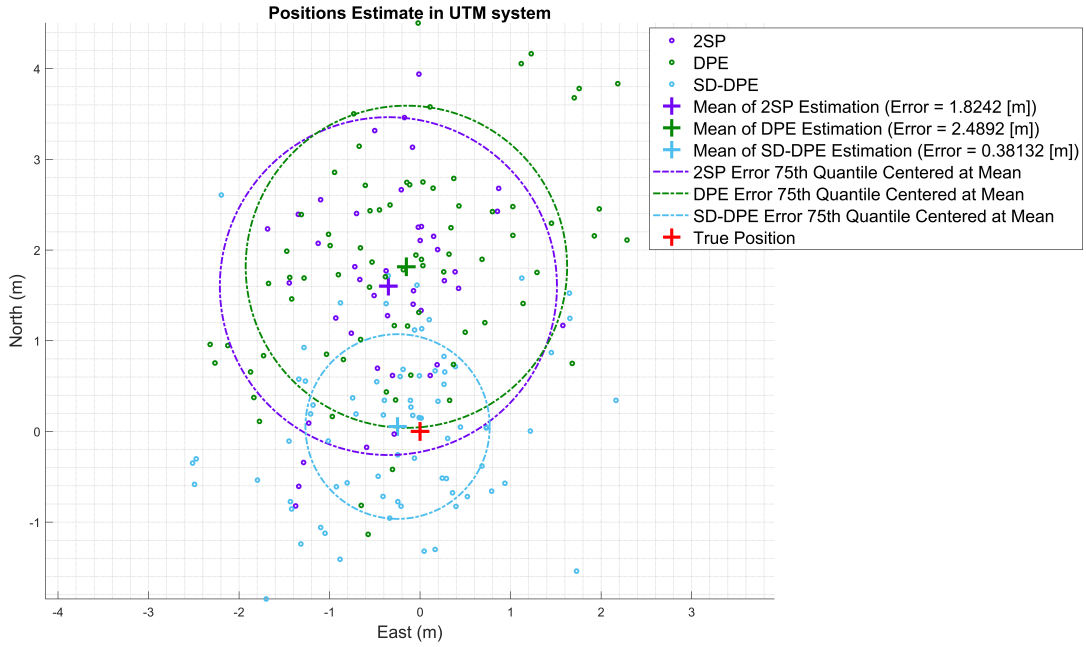

Figure 3: Comparison of positioning performance among 2SP, DPE and SD-DPE based on the over-the-air signal and real-world experiment settings. The origin stands for the true position in local UTM coordinates. The circles on the plot denotes the 75th quantile of the positioning error, centered at the mean of their estimation, to show the bias caused by iono/troposphere error.

3. Over-the-air Experiment

In this subsection, we implemented the proposed SD-DPE method with the over-the-air GNSS signal samples from the real world. A static Labsat GNSS signal recorder located on a rooftop ($41°32'23.85''$N, $2°6'49.41''E$ near Barcelona) was considered as the rover receiver. It sampled the GPS L1 signal at 25.375MHz with an intermediate frequency of 36.89Hz. GPS satellites $\{8, 10, 27, 30\}$ were continuously tracked during the 75-second record. Each satellite had a carrier-to-noise density ratio (C/N_0) ranging from 35 to 41 dB-Hz. The observation Rinex data from a zero-baseline reference station was provided by a Septentrio PolaEx-5e receiver at a rate of 1 Hz. Further experimental details can be found in [Liu et al., 2020].

Fig. 3 compares the positioning results of 2SP, DPE and SD-DPE. The origin is centered at the true position of the rover receiver. The 2SP method was implemented by GNSS-SDR [Fernandez-Prades et al., 2011, Pany et al., 2024]. It has less positioning points since the GNSS-SDR needs the first couple of seconds to decode the navigation bit. To enable the precise positioning and appeal the bias caused by iono/troposphere error, we implemented 20ms coherent integration for all approaches. We plot the 75th quantile of the positioning errors centered on their means to show the solution range of each approach under local East-North-Up coordinates. It is shown that the 2SP and DPE have the same positioning performance and bias without SD scheme, while SD-DPE obtains more accuracy by correcting the iono/troposphere error.

IV. CONCLUSION

This paper proposed the so-called SD-DPE approach as an extension of the DPE approach by including the DGPS technique. The core idea is that the CAF between two receivers can be modeled as the function of the difference of delay/pseudorange for each common satellite, and further the function of the baseline vector. We then proposed a signal reconstruction method to decrease the noise floor of CAF, which gives the SD-DPE cost function in Eq.(14). We provided the simulations of SD-DPE under different conditions and compared its performance with the standard DPE method. We also implemented the real-world experiment with the over-the-air signal. Both of the simulation and experiment showed that the proposed SD-DPE can effectively correct the iono/troposphere error and achieve better accuracy.

ACKNOWLEDGEMENTS

This work has been partially supported by the National Science Foundation under Awards ECCS-1845833 and CCF-2326559.

REFERENCES

[Appel et al., 2004] Appel, M., Labarre, R., and Radulovic, D. (2004). On accelerated random search. *SIAM Journal on Optimization*, 14(3):708–731.

[Arribas et al., 2010] Arribas, J., Closas, P., and Fernández-Prades, C. (2010). Joint acquisition strategy of GNSS satellites for computational cost reduction. In *2010 5th ESA Workshop on Satellite Navigation Technologies and European Workshop on GNSS Signals and Signal Processing (NAVITEC)*, pages 1–8. IEEE.

[Borio, 2008] Borio, D. (2008). A statistical theory for GNSS signal acquisition. *PHD Dissertation Polytecnico di Torino*.

[Borre et al., 2007] Borre, K., Akos, D. M., Bertelsen, N., Rinder, P., and Jensen, S. H. (2007). *A software-defined GPS and Galileo receiver: a single-frequency approach*. Springer Science & Business Media.

[Chu et al., 2019] Chu, A. H.-P., Chauhan, S. V. S., and Gao, G. X. (2019). GPS multireceiver direct position estimation for aerial applications. *IEEE Transactions on Aerospace and Electronic Systems*, 56(1):249–262.

[Closas et al., 2007] Closas, P., Fernández-Prades, C., and Fernández-Rubio, J. A. (2007). Maximum likelihood estimation of position in GNSS. *IEEE Signal Processing Letters*, 14(5):359–362.

[Closas et al., 2009] Closas, P., Fernández-Prades, C., and Fernández-Rubio, J. A. (2009). Direct position estimation approach outperforms conventional two-steps positioning. In *2009 17th European Signal Processing Conference*, pages 1958–1962. IEEE.

[Closas and Gusi-Amigo, 2017] Closas, P. and Gusi-Amigo, A. (2017). Direct position estimation of gnss receivers: Analyzing main results, architectures, enhancements, and challenges. *IEEE Signal Processing Magazine*, 34(5):72–84.

[Dampf et al., 2019] Dampf, J., Lichtenberger, C. A., and Pany, T. (2019). Probability analysis for Bayesian direct position estimation in a real-time GNSS software receiver. In *Proceedings of the 32nd International Technical Meeting of the Satellite Division of The Institute of Navigation (ION GNSS+ 2019)*, pages 3543–3566.

[Elsobeiey and El-Rabbany, 2014] Elsobeiey, M. and El-Rabbany, A. (2014). Efficient between-satellite single-difference precise point positioning model. *Journal of surveying engineering*, 140(2):04014007.

[Fernandez-Prades et al., 2011] Fernandez-Prades, C., Arribas, J., Closas, P., Aviles, C., and Esteve, L. (2011). GNSS-SDR: An open source tool for researchers and developers. In *Proceedings of the 24th International Technical Meeting of The Satellite Division of the Institute of Navigation (ION GNSS 2011)*, pages 780–794.

[Gao et al., 2022] Gao, Y., Gao, Y., Jiang, Y., and Liu, B. (2022). A modified between-receiver single-difference-based fault detection and exclusion algorithm for real-time kinematic positioning. *IET Radar, Sonar & Navigation*, 16(8):1269–1281.

[Groves, 2013] Groves, P. (2013). *Principles of GNSS, Inertial, and Multisensor Integrated Navigation Systems, Second Edition*. Artech.

[Gusi-Amigó et al., 2014] Gusi-Amigó, A., Closas, P., Mallat, A., and Vandendorpe, L. (2014). Cramér-rao bound analysis of UWB based localization approaches. In *2014 IEEE International Conference on Ultra-WideBand (ICUWB)*, pages 13–18. IEEE.

[Gusi-Amigó et al., 2018] Gusi-Amigó, A., Closas, P., Mallat, A., and Vandendorpe, L. (2018). Ziv-Zakai bound for direct position estimation. *NAVIGATION, Journal of the Institute of Navigation*, 65(3):463–475.

[Hofmann-Wellenhof et al., 2007] Hofmann-Wellenhof, B., Lichtenegger, H., and Wasle, E. (2007). *GNSS–global navigation satellite systems: GPS, GLONASS, Galileo, and more*. Springer Science & Business Media.

[Kaplan and Hegarty, 2017] Kaplan, E. D. and Hegarty, C. (2017). *Understanding GPS/GNSS: principles and applications*. Artech house.

[Langley, 1998] Langley, R. B. (1998). Rtk gps. *Gps World*, 9(9):70–76.

[Liu et al., 2020] Liu, X., Ribot, M. Á., Gusi-Amigó, A., Closas, P., Garcia, A. R., and Subirana, J. S. (2020). RTK feasibility analysis for GNSS snapshot positioning. In *Proceedings of the 33rd International Technical Meeting of the Satellite Division of The Institute of Navigation (ION GNSS+ 2020)*, pages 2911–2921.

[Liu et al., 2004] Liu, X., Tiberius, C., and de Jong, K. (2004). Modelling of differential single difference receiver clock bias for precise positioning. *GPS Solutions*, 7:209–221.

[Morton et al., 2021] Morton, Y. J., van Diggelen, F., Spilker Jr, J. J., Parkinson, B. W., Lo, S., and Gao, G. (2021). *Position, Navigation, and Timing Technologies in the 21st Century: Integrated Satellite Navigation, Sensor Systems, and Civil Applications*. John Wiley & Sons.

[Pany et al., 2024] Pany, T., Akos, D., Arribas, J., Bhuiyan, M. Z. H., Closas, P., Dovis, F., Fernandez-Hernandez, I., Fernández-Prades, C., Gunawardena, S., Humphreys, T., et al. (2024). GNSS Software-Defined Radio: History, Current Developments, and Standardization Efforts. *NAVIGATION: Journal of the Institute of Navigation*, 71(1).

[Tang et al., 2023] Tang, S., Li, H., Calatrava, H., and Closas, P. (2023). Precise direct position estimation: Validation experiments. In *2023 IEEE/ION Position, Location and Navigation Symposium (PLANS)*, Monterey, CA.

[Tsui, 2005] Tsui, J. B.-Y. (2005). *Fundamentals of global positioning system receivers: a software approach*. John Wiley & Sons.

[Vicenzo et al., 2023] Vicenzo, S., Xu, B., Dey, A., and Hsu, L.-T. (2023). Experimental Investigation of GNSS Direct Position Estimation in Densely Urban Area. In *Proceedings of the 36th International Technical Meeting of the Satellite Division of The Institute of Navigation (ION GNSS+ 2023)*, pages 2906–2919.

[Xiao et al., 2016] Xiao, L., Li, X., and Zeng, Y. (2016). Gnss spoofing detection using pseudo-range single difference between two receivers. In *2017 2nd International Conference on Machinery, Electronics and Control Simulation (MECS 2017)*, pages 292–298. Atlantis Press.